Infrared A Radiation Promotes Survival of Human Melanocytes Carrying Ultraviolet Radiation-Induced DNA Damage

S. Kimeswenger[1], **A. Schwarz**[2], **D. Födinger**[1], **S. Müller**[2], **H. Pehamberger**[1], **T. Schwarz**[2], and **C. Jantschitsch**[1]

[1]Division of General Dermatology, Department of Dermatology, Medical University of Vienna, Austria

[2]Department of Dermatology, Christian-Albrechts-University Kiel, Germany

Abstract

The link between solar radiation and melanoma is still elusive. Although infrared radiation (IR) accounts for over 50% of terrestrial solar energy, its influence on human skin is not well explored. There is increasing evidence that IR influences the expression patterns of several molecules independently of heat. A previous *in vivo* study revealed that pre-treatment with IR might promote the development of UVR-induced non-epithelial skin cancer and possibly of melanoma in mice. To expand on this, the aim of the present study was to evaluate the impact of IR on UVR-induced apoptosis and DNA repair in normal human epidermal melanocytes. The balance between these two effects is a key factor of malignant transformation. Human melanocytes were exposed to physiologic doses of IR and UVR. Compared to cells irradiated with UVR only, simultaneous exposure to IR significantly reduced the apoptotic rate. However, IR did not influence the repair of UVR-induced DNA damage. IR partly reversed the pro-apoptotic effects of UVR via modification of the expression and activity of proteins mainly of the extrinsic apoptotic pathway. In conclusion, IR enhances the survival of melanocytes carrying UVR-induced DNA damage and thereby might contribute to melanomagenesis.

Keywords

Ultraviolet radiation; infrared radiation; melanocytes; apoptosis; DNA damage

Introduction

Although melanomas account for only five percent of skin cancers, they are responsible for 80 percent of skin cancer-related deaths (1). Over the last decades melanoma rates have been growing in many countries (2), leading to an increase in studies investigating the impact of environmental factors on melanomagenesis. However, the exact relationship between

Corresponding Author: Dr. Christian Jantschitsch, Department of Dermatology, Medical University of Vienna, Waehringer Guertel 18-20, A-1090 Vienna, Austria, Telephone: +43-1-40400-77020, Fax: +43-1-40400-76990, christian.jantschitsch@meduniwien.ac.at.

Conflict of Interest
The authors declare no conflict of interest.

exposure to sunlight and melanoma formation is not well understood and still a controversial issue (3).

If exposed to natural sunlight, human skin is not only affected by ultraviolet-B (UVB, 290–320 nm), ultraviolet-A radiation (UVA, 320–400 nm), and visible light (VIS, 400–760 nm) but also by infrared radiation (IR, 780–1,000,000 nm) which accounts for the majority of solar energy reaching the earth's surface (54.3%). Within IR, the infrared-A (IRA) portion (780–1,400 nm) is the predominant terrestrial spectrum (4–6). So far most investigators have focused on the influence of UVR on melanomagenesis. A possible role of IR in this context has barely been considered. This is surprising since i) IR is the predominant portion of terrestrial solar energy, ii) upon exposure to natural sunlight UVR and IR are highly correlated, and iii) all epidemiological studies addressing the impact of natural sun exposure on melanoma implicate not only effects of UVR but also those of IR.

There is accumulating evidence that IR exerts biological effects independent of heat (7, 8). Similar to UVR, IRA is thought to be involved in premature skin aging (9). Although IRA alone is not carcinogenic, it is suspected to have a modifying effect on UVR-induced carcinogenesis (8, 10, 11). In recent years, several molecular pathways within cells have been shown to be affected by IR exposure (7, 8). In addition, there is increasing evidence that biological effects of different wavebands of the solar spectrum influence each other (10, 12). The impact of these interactions on human skin is still poorly understood.

In human skin besides UVR also IR induces ROS (13). While ROS induced by IR are mainly produced in the mitochondria (IR is absorbed by complex IV of the mitochondrial respiration chain), UVR-induced ROS have been detected in the cytoplasm (14, 15). As UVR might be absorbed by mitochondrial DNA, there is also evidence that UVR is capable of producing ROS in the mitochondria (16). In human melanocytes, ROS balance might be of particular importance, since i) ROS are supposed to be involved in melanomagenesis (17) and ii) pheomelanin is a known pro-oxidative agent (18) which has recently been confirmed to function as a carcinogen in melanocytes independently of UVR (19, 20).

UVR-mediated apoptosis is a protective mechanism preventing malignant transformation by eliminating cells carrying high loads of UVR-induced DNA damage (21). UVR can induce apoptosis at least via three different mechanisms: i) Induction of the extrinsic pathway of apoptosis by activating the death receptor CD95/Fas, ii) activation of the intrinsic pathway which is triggered mainly by DNA damage and iii) generation of ROS (22).

Melanocytes, the precursor cells of melanoma, have one special phenotypic trait distinguishing them from all other cell types, the ability to produce melanin (23, 24). The mutation spectrum of melanoma is somewhat different to that of non-melanoma skin cancer (25). Unlike squamous cell carcinomas, melanomas cannot be induced *in vivo* in normal mice by exclusive exposure to UVR. In contrast, hepatocyte growth factor transgenic mice develop melanomas upon a single neonatal UV exposure (26). Transgenic mice carrying the V600E BRAF mutation which is present in around 50% of all human melanomas (27) develop spontaneously melanomas but the development can be accelerated as well as the number of melanomas increased upon repetitive UVR exposure (28). In addition, metastasis

of melanomas, which develop spontaneously in the HGF-CDK4 (R24C9) transgenic mouse model, is enhanced upon UVR exposure (29). Since in all these models a transgenic oncogene mutation is an absolute requirement for the development of melanomas which then can be promoted by UVR it is concluded that UVR on its own is not able to induce melanomas but just plays an adjuvant, though clinically relevant role.

When studying the effect of IRA on UVR-induced carcinogenesis *in vivo*, our primary read-out systems were the time until tumor occurrence and the frequency of squamous cell carcinomas. Surprisingly, we observed a change in the tumor types induced by UVB and IRA which included two melanomas (13% of all tumors in this group). In mice exposed to only UVB or only IRA no melanomas were detected (11). Since in this setting wild type mice and not transgenic ones were used and UVB plus IRA was the only exogenous stimulus to induce the melanomas, we were interested to further study the effect of IRA in combination with UVB on melanocytes. In particular we were interested to evaluate the impact of IRA on UVR-induced apoptosis and DNA repair in normal human epidermal melanocytes (NHEM).

Methods

Cells and reagents

Normal human epidermal melanocytes (NHEM) of three different neonatal donors (all Caucasians) were obtained from CellSystems (St. Katharinen, Germany) and cultured in DermaLife® Basal Medium with Supplements (CellSystems).

Irradiation of cells

Prior to irradiation medium was replaced by PBS. Subconfluent cells were exposed to a dose of 250 J/cm^2 water-filtered IRA and/or to 0.40 J/cm^2 UVB (0.08 J/cm^2 UVB for DNA damage experiments). During irradiation, temperature of PBS was maintained stable (25°C) using a water-cooled board (Hoefer Scientific, Holliston, MA). After irradiation PBS was replaced by the previously preserved melanocyte medium.

As a source for IRA served a Hydrosun®750 water-filtered IRA lamp (Hydrosun, Mühlheim, Germany) equipped with a 760 nm cut-off filter emitting between 760 and 1440 nm. IRA dosimetry was performed using a HBM1 infrared exposure measurement device (Hydrosun).

As a source for UVR served a Mutzhas Supersun 5000 Solar Simulator equipped with a UVB lamp emitting light in the range of 290–330 nm (Mutzhas, Essen, Germany). The UVR dosimetry was carried out using an IL1700 research radiometer (International light, Newburyport, MA) with a SED240#3143detector/NS313#12178 filter measuring the flux at 313 nm.

Detection of apoptosis

Cell death detection assay—24 hours after stimulation, cells were trypsinized and dissolved from dishes, counted and analyzed according to the manufacturer's protocol by a cell death detection ELISA (Cell death detection ELISA^{plus}, Roche Molecular

Biochemicals, Mannheim, Germany). The enrichment of mono- and oligonucleosomes released into the cytoplasm of cell lysates was detected by biotinylated anti-histone- and peroxidase-coupled anti-DNA antibodies.

Annexin staining—24 hours after irradiation, cells were trypsinized, resuspended in Annexin buffer (containing HEPES, NaCl and $CaCl_2$). Consequently, cells were stained with Propidium Iodide Staining Solution, FITC-Annexin (both eBioscience, Vienna, Austria) or both. After ten minutes of incubation in the dark, the proportions of apoptotic and necrotic cells of 20.000 cells were evaluated by FACS analysis (FACSCalibur™, Becton Dickinson, Heidelberg, Germany) and CellQuest™ Pro software (BD, version 0.3.af3b).

Evaluation of DNA repair

Southwestern slot-blot analysis—Six hours after exposure genomic DNA was isolated from $\sim10^6$ cells according to the Puregene DNA extraction protocol (Gentra Systems, Minneapolis, MI). Non-denatured DNA (1 µg) was transferred to a positively charged nylon membrane by vacuum slot blotting and fixed by baking the membrane for 60 minutes at 80°C. A monoclonal antibody directed against thymine dimers (Kamiya Biomedical Company, Seattle, WA) was used for Southwestern analysis. Detection was carried out with an ECL™ Anti-Mouse IgG, Horseradish Peroxidase-Linked Species-Specific Whole Antibody (Amersham, Uppsala, Sweden). To ensure equal distribution of DNA, stripping and consecutive incubation with an antibody against adenosine (WAK-Chemie, Steinbach, Germany) was performed.

Shuttle Vector Assay—The 4,465 bp pCAT3-control vector (Promega Corp., Madison, WI) containing the gene for chloramphenicol acetyl transferase (CAT) as an insert was irradiated with 0.06 J/cm^2 UVB. UVR-damaged plasmid (50 µg) was electroporated into $\sim1x10^6$ untreated or IRA exposed (250 J/cm^2) NHEM using a GenePulser Xcell electroporator (Bio-Rad, Hercules, CA). 16 hours later, CAT-enzyme activity was measured. Cells were harvested, proteins were purified according to a standard protocol, and the protein concentration was determined using the BCA method. Equal amounts of total protein were subjected to a CAT-ELISA (Roche Molecular Biochemicals).

Protein expression/activity analysis

Flow cytometry—Standard protocols were used for intra- and extracellular FACS staining. 24 hours after irradiation, cells were harvested, fixed and permeabilized using BD Cytofix/Cytoprem Fixation/Permeabilization Kit (BD Biosciences, Heidelberg, Germany). Melanocytes were incubated with the following first antibodies: Rabbit anti-human/mouse FLIP$_L$ (R&D Systems, Minneapolis, MN); mouse Alexa Fluor 488 anti-human Bcl-2; rat anti-human BID (both Biolegend, Fell, Germany) and rabbit anti-human BAX (BD Biosciences, Heidelberg, Germany). Respective FITC-conjugated second step antibodies were used: FITC-conjugated goat anti-rat, (Biomeda, Burlingame, CA) and FITC Alexa 488 conjugated goat anti-rabbit (Molecular Probes, LifeTechnologies, Vienna, Austria). For extracellular staining of CD95 a mouse FITC conjugated anti-human CD95 antibody (Ancell Corporation, Bayport, MN) was used. Analysis was performed using a FC500 flow cytometer (Beckman Coulter, Krefeld, Germany) and a BD FACSCalibur™ (Becton

Dickinson, Heidelberg, Germany) and CXP 2.2 software as well as CellQuestTM Pro software (BD, verson 0.3.af3b)

Measurement of caspase activity—24 hours after irradiation, activities of caspases 8 and 9 were determined using commercially available assay kits (Calbiochem/Merck, Darmstadt, Germany). Cells were harvested and proteins purified. Caspase-8 and caspase-9 activities were determined according to the manufacturer's protocol. Slopes were calculated from the fluorescence (λ_{em}=400 nm, λ_{ex}=505 nm) measured immediately, after one hour and after two hours, normalized to untreated cells (= control), which was arbitrarily set as one.

Statistical analysis

Each experiment was performed independently at least three times for each of the three different Caucasian donors, except expression analyses (CD95, BID, BAX, Bcl-2, FLIP$_L$) which were conducted using NHEM of two different Caucasian donors. Statistical analysis was performed using paired or unpaired, two-tailed Student's t-test (depending on the type of experiment) and Grubb's test for outliers. Differences were considered significant at $p < 0.05$.

Results

Simultaneous exposure to IRA reduces UVB-induced apoptosis

In NHEM simultaneously exposed to 250 J/cm^2 of IRA, a significant reduction of UVB-induced apoptosis was observed (Figure 1a). The apoptotic rate was determined 24 hours after exposure to IRA and/or UVB (0.40 J/cm^2) using a cell death detection ELISA. IRA alone did not influence the apoptotic rate. The temperature of PBS in the dishes of all conditions did not exceed 25 °C.

In order to confirm these results, the levels of apoptosis and necrosis were determined by FACS analysis using Annexin V and Propidium Iodide staining 24 hours after exposure. In agreement with the cell death detection ELISA data, simultaneous irradiation of NHEM with IRA and UVB significantly reduced UVB-induced apoptosis (Figure 1b,c)

IRA does not influence the repair of UVB-induced DNA damage

Since a major trigger of UVR-induced apoptosis is DNA damage generated by UVR (30), the effect of IRA on the repair of UVB-induced DNA damage was determined. Six hours after exposure of NHEM to UVB and/or IRA, the amount of cyclobutane pyrimidine dimers (CPD) was visualized using Southwestern slot blot analysis. We observed equal amounts of DNA damage in cells exposed to UVB and to UVB + IRA simultaneously (Figure 2a), indicating that IRA does not influence the repair of UVB-damaged DNA. Similar experiments with identical results were performed at 24 and 48 hours after irradiation (Figure 2b). In addition, we excluded differences in the initial amount of DNA damage in the UVB and IRA+UVB group by determining the amount of CPDs immediately after irradiation (Figure 2b).

In order to consolidate these findings, a shuttle vector assay was employed. A UVB-treated and hence DNA-damaged reporter construct containing the CAT gene was transfected into NHEM which were either exposed to IRA immediately after transfection or remained untreated. In order to determine the efficiency of DNA repair CAT expression was evaluated 20 hours after transfection using FACS analysis. No difference with regard to the amount of CAT expression per μg of protein between IRA exposed and untreated melanocytes was detected (Figure 2c). This indicates equal amounts of DNA damage 20 hours after transfection and hence confirms that in NHEM IRA does not affect DNA repair.

IRA partly inhibits the UVB-induced extrinsic apoptotic pathway, but does not influence the intrinsic apoptotic pathway

UVB alone significantly increased caspase-8 activity, whereas simultaneous exposure to IRA partly inhibited UVB-induced elevation of caspase-8 activity (Figure 3a). In contrast, simultaneous irradiation of NHEM with IRA and UVB resulted in a similar caspase-9 activity as in NHEM exposed to UVB only (Figure 3b). This indicates that while IRA influences the extrinsic apoptotic pathway (caspase-8), it has no effect on the intrinsic apoptotic pathway (caspase-9). Thus, IRA appears to reduce UVB-induced apoptosis merely via its influence on the extrinsic apoptotic pathway.

IRA reduces UVB-induced apoptosis via a modification of the expression of apoptosis-related proteins

UVB is capable of activating the extrinsic pathway of apoptosis via increased expression and multimerization of the death receptor CD95 (22, 31). The simultaneous exposure to IRA blocked UVB-induced up-regulation of pro-apoptotic CD95 (Figure 4).

The downstream caspase of CD95 is caspase-8, which after activation either directly induces apoptosis through processor caspases (type I) or activates pro-apoptotic BID and the mitochondrial pathway (type II) (32). Intracellular antibody staining and subsequent FACS analysis revealed that simultaneous exposure of NHEM to IRA inhibited UVB-induced up-regulation of BID (Figure 4).

$FLIP_L$ is an enzyme preventing caspase-8 activation and thus acts anti-apoptotic (33). IRA partly restored UVB-induced down-regulation of $FLIP_L$ which was significantly reduced after exposure to UVB alone (Figure 4).

Moreover, UVB-mediated down-regulation of anti-apoptotic Bcl-2 was partly restored by simultaneous exposure to IRA (Figure 4). Bcl-2 interacts with BAX and prevents BAX from activating mitochondria-mediated apoptosis (34). Accordingly, IRA reduced the expression of pro-apoptotic BAX in NHEM exposed to UVB + IRA compared to only UVB (data not shown).

Discussion

A variety of studies have been conducted addressing the role on the action of UVR in the pathogenesis of melanoma, while to our knowledge there are no studies adressing the influence of IR on melanomagenesis. Although IR is the predominant terrestrial solar

waveband which under natural conditions is delivered in combination with UVR, it has barely been considered in this context (4). To our surprise, additional exposures to IRA induced melanomas in wild type C57BL/6 mice undergoing a conventional long term UVR irradiation protocol (11). Although this was observed incidentally only in a few mice, we were interested to further persue this issue on a molecular level.

To expand on this, in the present study, the impact of IR on UVR-induced apoptosis and DNA repair in normal epidermal human melanocytes was evaluated. We show that in human melanocytes simultaneous exposure to IRA significantly reduced UVR induced apoptosis. This is in accordance with preceding studies showing that pre-treatment with IRA reduced UVB-induced apoptosis in primary murine keratinocytes (10) and normal human dermal fibroblasts (35, 36). Noteworthy, the present study was performed in human melanocytes, and cells were exposed to IRA and UVB simultaneously, whereas in the preceding studies cells were treated with IRA prior to UVR (35).

In contrast to murine keratinocytes and human fibroblasts, in human melanocytes simultaneous exposure to IRA and UVB does not influence the repair of UVB-induced DNA damage. Since DNA damage caused by UVR is a major contributor to UVR-induced apoptosis, this indicates that in human melanocytes the anti-apoptotic effect of IRA is not caused by an influence on the nucleotide excision repair (NER).

DNA damage leads to an activation of the intrinsic apoptotic pathway in a *p53*- dependent manner (22). Consistently, we show that in human melanocytes IRA does not influence UVB-induced activation of caspase-9, a major mediator of the intrinsic apoptotic pathway. In contrast, IRA reduces UVB-induced activation of caspase-8 which is activated during the death receptor CD95L/FADD-mediated extrinsic apoptotic pathway. Since, on the other hand, in murine keratinocytes as well as human fibroblasts IRA partly inhibits UVB-mediated activation of both caspase-8 and caspase-9 (10), the effects of IRA in different cell types might involve different apoptotic pathways: In primary murine keratinocytes and human dermal fibroblasts IRA influences both the extrinsic and intrinsic apoptotic pathway, whereas in human melanocytes IRA interferes with the extrinsic apoptotic pathway only.

The divergent impact of IRA on the repair of UVR-induced DNA damage in keratinocytes, fibroblasts and melanocytes might be related to their different sensitivity to UVR (37). It is known that UVR-induced oxidative alterations and in particular oxidative DNA damage, are significantly more frequent in melanocytes than in keratinocytes (37, 38). Moreover, it cannot be excluded that melanin acts as chromophore for IRA and thus is involved in the anti-apoptotic effect of IRA.

In NHEM, IRA influences the extrinsic apoptotic pathway in several ways: i) IRA partly inhibits UVB-induced activation of caspase-8. ii) IRA prevents UVB-mediated up-regulation of CD95 expression. iii) IRA blocks UVB-induced up-regulation of the pro-apoptotic molecules BID and BAX. iiii) IRA partly antagonizes UVB-mediated down-regulation of the anti-apoptotic Bcl-2 and $FLIP_L$ proteins. Taken together, IRA partly blocks UVB-induced activation of the extrinsic apoptotic pathway via interfering with type I signaling

(inhibition of UVB-induced activation of caspase-8) as well as type II signaling (inhbition of UVB-induced up-regulation of BID) (33).

The anti-apoptotic molecule $FLIP_L$ prevents caspase-8 activation (33). $FLIP_L$ has been reported to be regulated by ROS (33, 39). Hydrogen peroxide (H_2O_2) down-regulates $FLIP_L$ by increasing its ubiquitination and hence degradation. On the other hand, superoxide (O_2^-) stabilizes $FLIP_L$ expression and thereby prevents death receptor signaling (33, 40). Thus, an increased intracellular $O_2^-:H_2O_2$ ratio might act anti-apoptotic (33). Schroeder and colleagues demonstrated that IRA, in contrast to UVR, induces superoxide (O_2^-) in the mitochondria (41).

The production of ROS is particularly high in melanocytes due to the process of melanin synthesis (17), and therefore the composition of ROS is very important in these cells. From this point of view, our data might be interpreted that simultaneous exposure of NHEM to IRA and UVB provides an anti-apoptotic $O_2^-:H_2O_2$ ratio (33). We observed that IRA partly restores UVB-induced downregulation of anti-apoptotic Bcl-2. Noteworthy, O_2^- has been shown to up-regulate Bcl-2 (33). This observation fosters the assumption that ROS might at least in part mediate the effects of IRA.

The influence of IRA on UVR-induced ROS in human melanocytes is subject to further investigations.

Although the majority of DNA damage induced by UVB are CPD and 6,4-photoproducts, UVB also produces oxidative DNA damage to some extent. It is known that oxidative DNA damage increases apoptosis (42). As we observed the opposite effect (in human melanocytes IRA reduced UVB-mediated apoptosis) we conclude that either IRA does not produce oxidative DNA damage or the oxidative DNA damage caused by IRA is in a range physiologically not relevant.

On top of that it has to be mentioned that very recently it has been shown that CPD are produced in melanocytes even after termination of exposure to UV, so called dark CPD (43). We did not directly investigate the production of dark CPD in our system. However, even if dark CPD were generated, they would not influence our results since the amount of CPD in UVB only and IRA+UVB exposed melanocytes was equal immediately as well as 6, 24, and 48 hours after irradiation (Figure 2a,b).

UVR-induced apoptosis is a protective mechanism preventing malignant transformation by eliminating cells which carry high loads of UVR-induced DNA damage. We demonstrate that IRA is able to reduce UVB-induced apoptosis in human melanocytes. The inhibitory effect of IRA on UVB-induced apoptosis is mediated by its interference with the extrinsic pathway of apoptosis. In human melanocytes, IRA partly reverses UVB-induced apoptosis by inhibition of the activation of caspase-8 and alteration of the expression level of several apoptosis-related proteins. Since IRA does not affect the repair of UVB-induced DNA damage, the enhanced survival of severely DNA-damaged melanocytes might support the accumulation of UVB-induced mutations, malignant transformation, and ultimately melanomagenesis.

Acknowledgments

Abbreviations used

CAT	Chloramphenicol Acetyl Transferase
CPD	Cyclobutane Pyrimidine Dimers
IR	Infrared Radiation
NHEM	Normal Human Epidermal Melanocytes
ROS	Reactive Oxygen Species
UVR	Ultraviolet Radiation

References

1. Bertolotto C. Melanoma: from melanocyte to genetic alterations and clinical options. Scientifica (Cairo). 2013; 2013:635203. [PubMed: 24416617]

2. Poirier, V. Mortality, Incidence and gender - Malignant Melanoma. National Cancer Intelligence Network; 2012.

3. Moan JE, Baturaite Z, Dahlback A, et al. Ultraviolet radiation and cutaneous malignant melanoma. Adv Exp Med Biol. 2014; 810:359–374. [PubMed: 25207376]

4. Akhalaya MY, Maksimov GV, Rubin AB, et al. Molecular action mechanisms of solar infrared radiation and heat on human skin. Ageing Res Rev. 2014; 16:1–11. [PubMed: 24742502]

5. Schieke SM, Schroeder P, Krutmann J. Cutaneous effects of infrared radiation: from clinical observations to molecular response mechanisms. Photodermatol Photoimmunol Photomed. 2003; 19:228–234. [PubMed: 14535893]

6. O'Leary RE, Diehl J, Levins PC. Update on tanning: More risks, fewer benefits. J Am Acad Dermatol. 2014; 70:562–568. [PubMed: 24388421]

7. Calles C, Schneider M, Macaluso F, et al. Infrared A radiation influences the skin fibroblast transcriptome: mechanisms and consequences. J Invest Dermatol. 2010; 130:1524–1536. [PubMed: 20130591]

8. Schieke S, Stege H, Kurten V, et al. Infrared-A radiation-induced matrix metalloproteinase 1 expression is mediated through extracellular signal-regulated kinase 1/2 activation in human dermal fibroblasts. J Invest Dermatol. 2002; 119:1323–1329. [PubMed: 12485435]

9. Kligman LH. Intensification of ultraviolet-induced dermal damage by infrared radiation. Arch Dermatol Res. 1982; 272:229–238. [PubMed: 7165330]

10. Jantschitsch C, Majewski S, Maeda A, et al. Infrared radiation confers resistance to UV-induced apoptosis via reduction of DNA damage and upregulation of antiapoptotic proteins. J Invest Dermatol. 2009; 129:1271–1279. [PubMed: 19037232]

11. Jantschitsch C, Weichenthal M, Maeda A, et al. Infrared radiation does not enhance the frequency of ultraviolet radiation-induced skin tumors, but their growth behaviour in mice. Exp Dermatol. 2011; 20:346–350. [PubMed: 21410765]

12. Schieke SM, Ruwiedel K, Gers-Barlag H, et al. Molecular crosstalk of the ultraviolet a and ultraviolet B signaling responses at the level of mitogen-activated protein kinases. J Invest Dermatol. 2005; 124:857–859. [PubMed: 15816846]

13. Grether-Beck S, Marini A, Jaenicke T, et al. Photoprotection of human skin beyond ultraviolet radiation. Photodermatol Photoimmunol Photomed. 2014; 30:167–174. [PubMed: 24433486]

14. Heck DE, Vetrano AM, Mariano TM, et al. UVB light stimulates production of reactive oxygen species: unexpected role for catalase. J Biol Chem. 2003; 278:22432–22436. [PubMed: 12730222]

15. Cadet J, Douki T, Ravanat JL. Oxidatively generated damage to cellular DNA by UVB and UVA radiation. Photochem Photobiol. 2014

16. Swalwell H, Latimer J, Haywood RM, et al. Investigating the role of melanin in UVA/UVB- and hydrogen peroxide-induced cellular and mitochondrial ROS production and mitochondrial DNA damage in human melanoma cells. Free Radic Biol Med. 2012; 52:626–634. [PubMed: 22178978]

17. Denat L, Kadekaro AL, Marrot L, et al. Melanocytes as instigators and victims of oxidative stress. J Invest Dermatol. 2014; 134:1512–1518. [PubMed: 24573173]

18. Cotter MA, Thomas J, Cassidy P, et al. N-acetylcysteine protects melanocytes against oxidative stress/damage and delays onset of ultraviolet-induced melanoma in mice. Clin Cancer Res. 2007; 13:5952–5958. [PubMed: 17908992]

19. Mitra D, Luo X, Morgan A, et al. An ultraviolet-radiation-independent pathway to melanoma carcinogenesis in the red hair/fair skin background. Nature. 2012; 491:449–453. [PubMed: 23123854]

20. Prota, G. Melanins and Melanogenesis. Academic Press; 1992.

21. Maddodi N, Setaluri V. Role of UV in cutaneous melanoma. Photochem Photobiol. 2008; 84:528–536. [PubMed: 18248502]

22. Kulms D, Schwarz T. Independent contribution of three different pathways to ultraviolet-B-induced apoptosis. Biochem Pharmacol. 2002; 64:837–841. [PubMed: 12213577]

23. Slominski A, Tobin DJ, Shibahara S, et al. Melanin pigmentation in mammalian skin and its hormonal regulation. Physiol Rev. 2004; 84:1155–1228. [PubMed: 15383650]

24. Slominski A, Zmijewski MA, Pawelek J. L-tyrosine and L-dihydroxyphenylalanine as hormone-like regulators of melanocyte functions. Pigment Cell Melanoma Res. 2012; 25:14–27. [PubMed: 21834848]

25. Tsai KY, Tsao H. The genetics of skin cancer. American Journal of Medical Genetics Part C: Seminars in Medical Genetics. 2004; 131C:82–92.

26. Noonan FP, Recio JA, Takayama H, et al. Neonatal sunburn and melanoma in mice. Nature. 2001; 413:271–272. [PubMed: 11565020]

27. Davies H, Bignell GR, Cox C, et al. Mutations of the BRAF gene in human cancer. Nature. 2002; 417:949–954. [PubMed: 12068308]

28. Viros A, Sanchez-Laorden B, Pedersen M, et al. Ultraviolet radiation accelerates BRAF-driven melanomagenesis by targeting TP53. Nature. 2014; 511:478–482. [PubMed: 24919155]

29. Bald T, Quast T, Landsberg J, et al. Ultraviolet-radiation-induced inflammation promotes angiotropism and metastasis in melanoma. Nature. 2014; 507:109–113. [PubMed: 24572365]

30. Kulms D, Dussmann H, Poppelmann B, et al. Apoptosis induced by disruption of the actin cytoskeleton is mediated via activation of CD95 (Fas/APO-1). Cell Death Differ. 2002; 9:598–608. [PubMed: 12032668]

31. Bang B, Rygaard J, Baadsgaard O, et al. Increased expression of Fas on human epidermal cells after in vivo exposure to single-dose ultraviolet (UV) B or long-wave UVA radiation. Br J Dermatol. 2002; 147:1199–1206. [PubMed: 12452871]

32. Barnhart BC, Alappat EC, Peter ME. The CD95 type I/type II model. Semin Immunol. 2003; 15:185–193. [PubMed: 14563117]

33. Subramaniam K, Hirpara JL, Tucker-Kellogg L, et al. FLIP: a flop for execution signals. Cancer Lett. 2013; 332:151–155. [PubMed: 22781394]

34. Oltvai ZN, Milliman CL, Korsmeyer SJ. Bcl-2 Heterodimerizes in-Vivo with a Conserved Homolog, Bax, That Accelerates Programmed Cell-Death. Cell. 1993; 74:609–619. [PubMed: 8358790]

35. Frank S, Oliver L, Lebreton-De Coster C, et al. Infrared radiation affects the mitochondrial pathway of apoptosis in human fibroblasts. J Invest Dermatol. 2004; 123:823–831. [PubMed: 15482467]

36. Menezes S, Coulomb B, Lebreton C, et al. Non-coherent near infrared radiation protects normal human dermal fibroblasts from solar ultraviolet toxicity. J Invest Dermatol. 1998; 111:629–633. [PubMed: 9764844]

37. Larsson P, Andersson E, Johansson U, et al. Ultraviolet A and B affect human melanocytes and keratinocytes differently. A study of oxidative alterations and apoptosis. Exp Dermatol. 2005; 14:117–123. [PubMed: 15679581]

38. Mouret S, Forestier A, Douki T. The specificity of UVA-induced DNA damage in human melanocytes. Photochem Photobiol Sci. 2012; 11:155–162. [PubMed: 21986862]

39. Wang L, Azad N, Kongkaneramit L, et al. The Fas death signaling pathway connecting reactive oxygen species generation and FLICE inhibitory protein down-regulation. J Immunol. 2008; 180:3072–3080. [PubMed: 18292530]

40. Peus D, Vasa RA, Meves A, et al. H2O2 is an important mediator of UVB-induced EGF-receptor phosphorylation in cultured keratinocytes. J Invest Dermatol. 1998; 110:966–971. [PubMed: 9620307]

41. Schroeder P, Pohl C, Calles C, et al. Cellular response to infrared radiation involves retrograde mitochondrial signaling. Free Radic Biol Med. 2007; 43:128–135. [PubMed: 17561101]

42. Tada-Oikawa S, Oikawa S, Kawanishi S. Role of ultraviolet A-induced oxidative DNA damage in apoptosis via loss of mitochondrial membrane potential and caspase-3 activation. Biochem Biophys Res Commun. 1998; 247:693–696. [PubMed: 9647755]

43. Premi S, Wallisch S, Mano CM, et al. Photochemistry. Chemiexcitation of melanin derivatives induces DNA photoproducts long after UV exposure. Science. 2015; 347:842–847. [PubMed: 25700512]
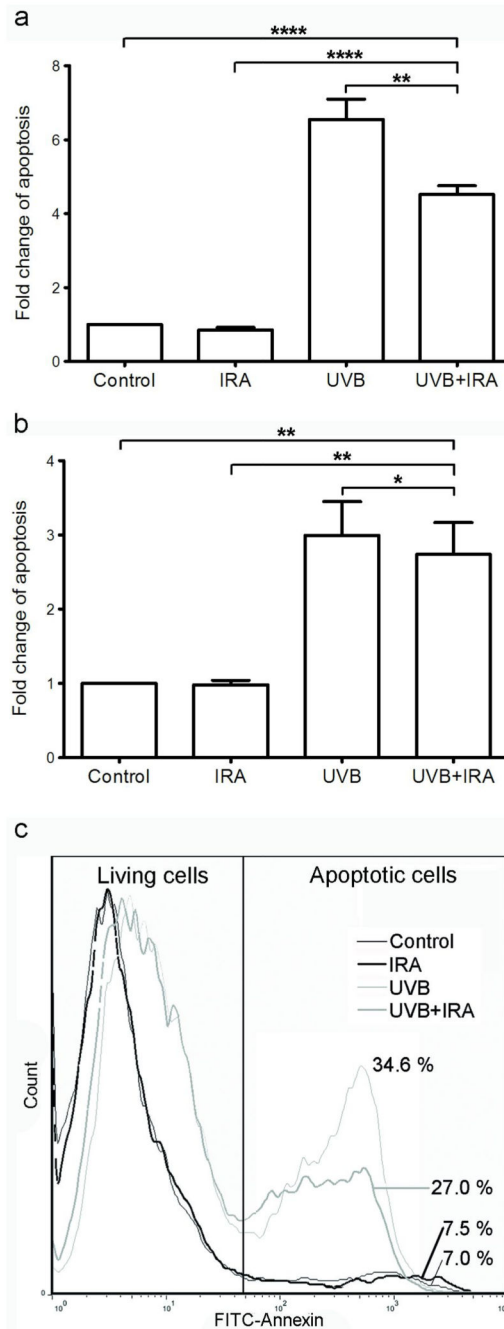
Figure 1. Simultaneous exposure to IRA significantly reduces UVB-induced apoptosis.
NHEM were exposed to 250 J/cm^2 IRA, 0.40 J/cm^2 UVB or IRA+UVB. 24 hours later cells were harvested and equal amounts of cells were subjected to a **(a)** cell death detection ELISA and **(b, c)** Annexin V/Propidium-Iodide staining and subsequent FACS analysis. **(a)** Data were normalized to untreated cells = Control which was arbitrarily set as 1. One representative experiment performed in triplicates out of 18 independently performed experiments using 3 different donors is shown. Error bars represent SD. ** p<0.005; **** p<0.00005 **(b)** Data were normalized to untreated cells = Control which was arbitrarily set

as 1. Cumulative data of three donors (n = 12). One outlier has been eliminated. Error bars represent SEM. *p<0.05; ** p<0.005. **(c)** Annexin V/Propidium Iodide staining results of one representative donor is shown. Histograms show fluorescence intensity (*x axis*) versus cell number (*y axis*). Percentages indicate apoptotic cells.
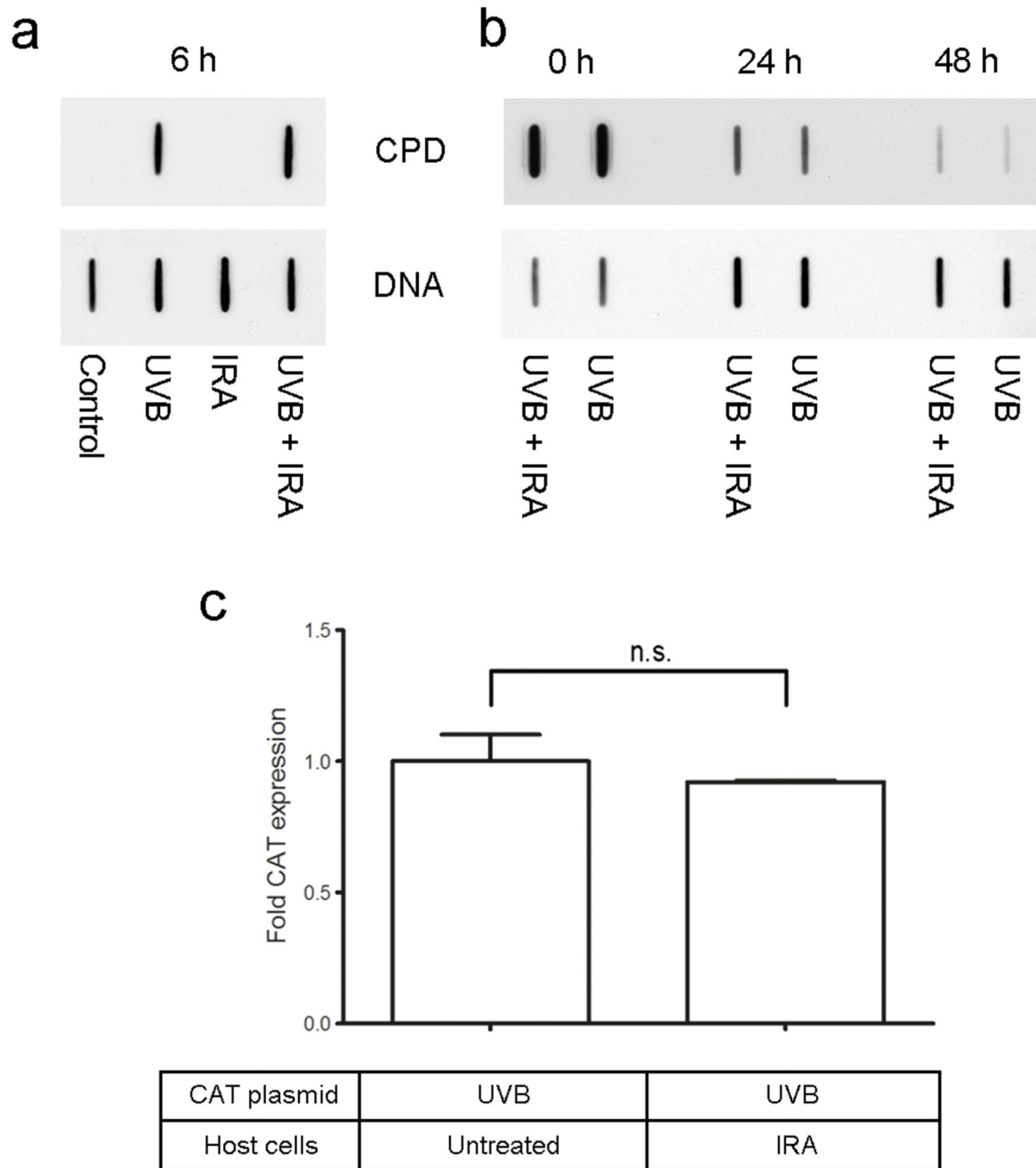
Figure 2. IRA has no impact on the repair of UVB-induced DNA damage.
(a+b) Southwestern slot(dot)-blot analysis using an antibody against CPD. Upper lane (CPD): Amount of CPD induced for each irradiation condition. Lower lane (DNA): Demonstrates equal distribution of DNA. Shown is one representative experiment. **(a)** 6, **(b)** 0, 24 and 48hours after simultaneous irradiation with 250 J/cm^2 IRA and 0.08 J/cm^2 UVB comparable amounts of CPD were observed in UVB and IRA+UVB irradiated NHEM. (c) Shuttle vector assay shows equal CAT-expression of cells transfected with UVB-exposed (0.06 J/cm^2) plasmid (containing the CAT gene) in cells treated with IRA (250 J/cm^2) or

untreated cells. Bars represent duplicates normalized to untreated cells which were set at 1. One representative out of 16 independently performed experiments using 3 different donors is shown. Error bars indicate SD. n.s. =not significant
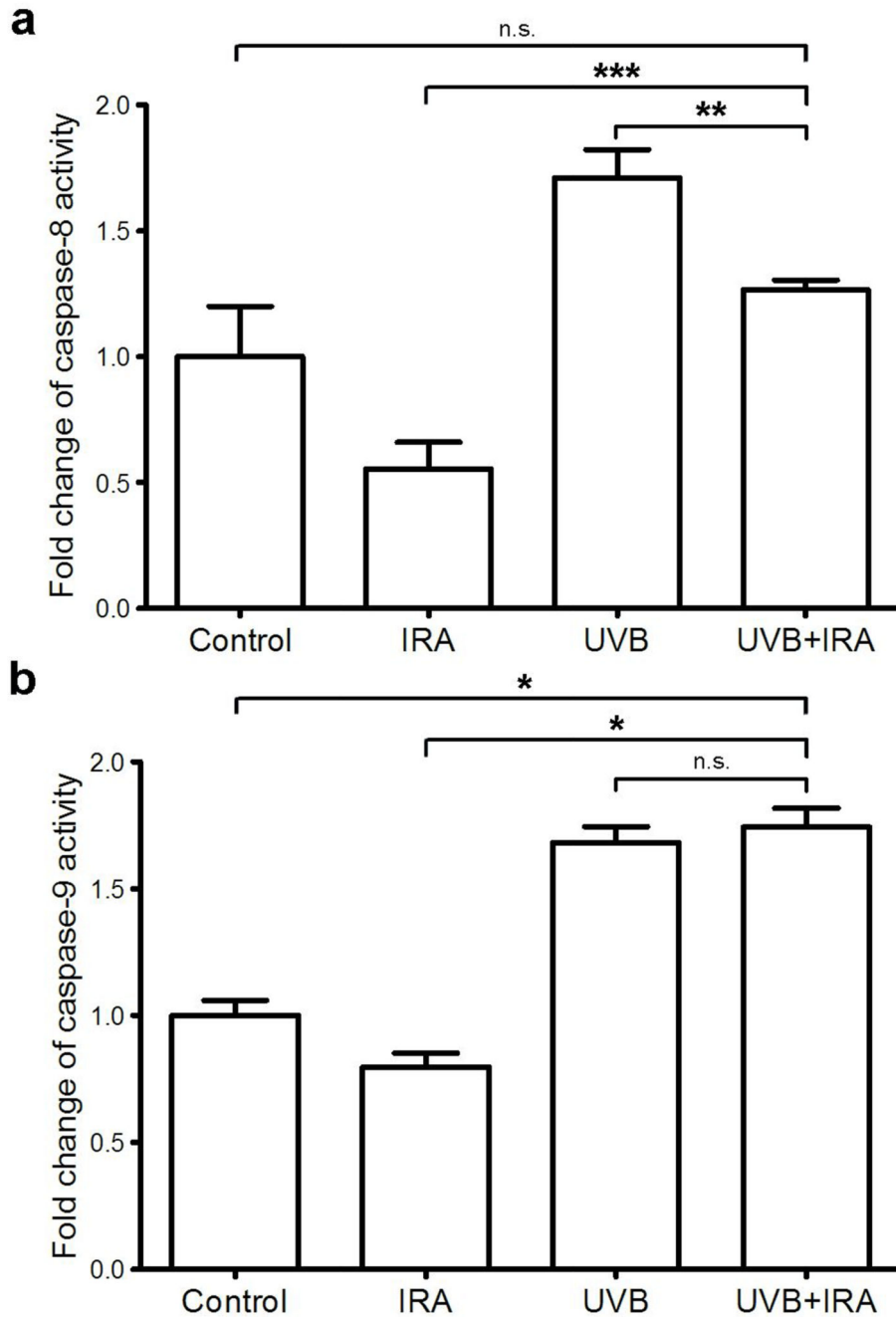
Figure 3. IRA partly inhibits UVB-mediated induction of caspase-8 but not caspase-9 activity. NHEM were exposed to 250 J/cm^2 IRA, 0.40 J/cm^2 UVB or IRA+UVB. 24 hours later cells were harvested. Caspase activities were determined by using respective caspase activity assays. Slopes of fluorescence were calculated and normalized to those of untreated cells which were arbitrarily set as 1. **(a)** Caspase-8 activity: Mean ± SD of triplicates of one representative experiment out of 3 independent experiments for each donor is shown; ** p<0.005; *** p<0.0005; n.s.=not significant **(b)** Caspase-9 activity: Mean ± SD of

duplicates of one representative experiment out of 3 independent experiments for each donor is shown; * p<0.05; n.s.=not significant.
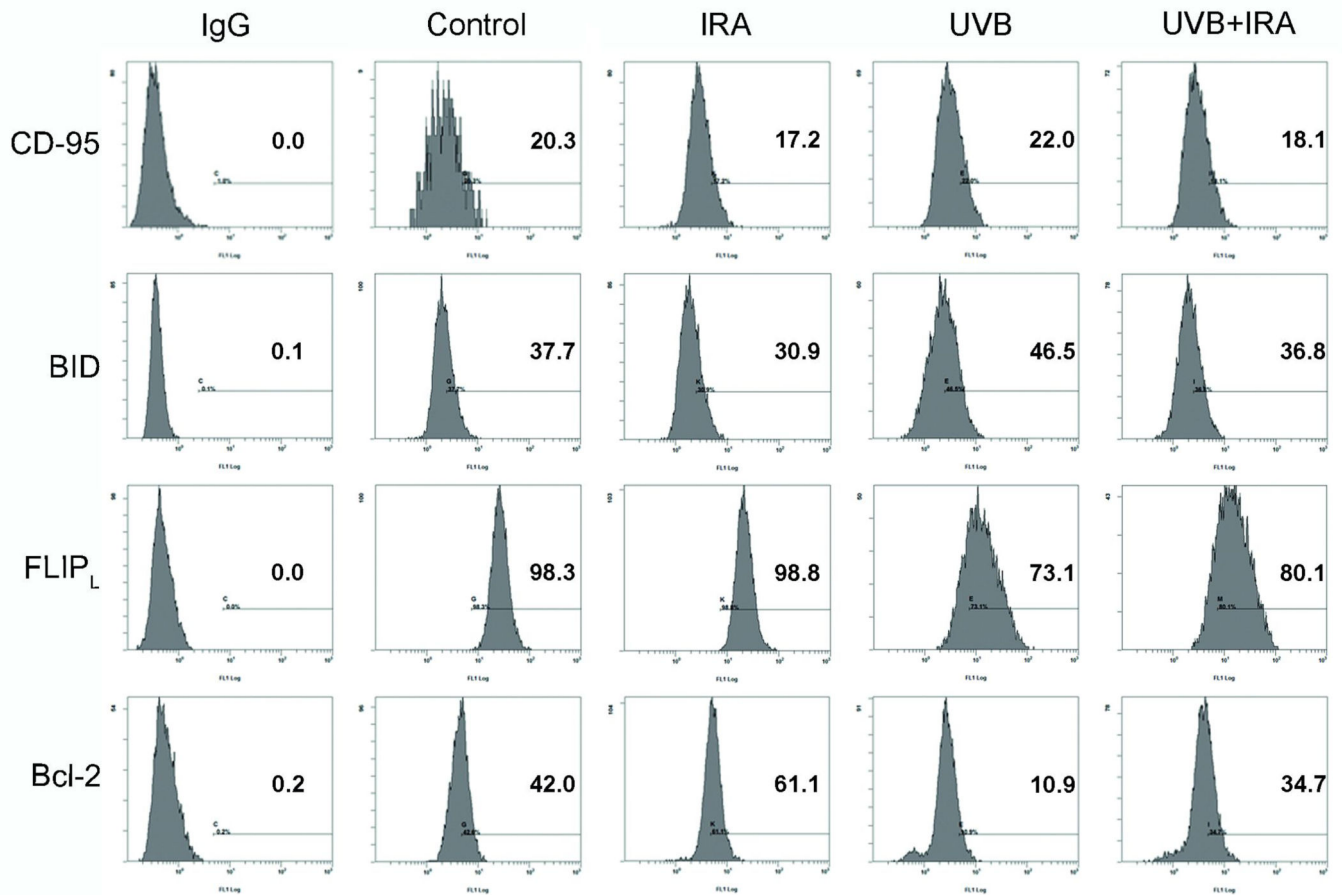
Figure 4. IRA alters the expression of pro- and anti-apoptotic proteins in UVB exposed human melanocytes.
NHEM were exposed to 250 J/cm^2 IRA, 0.40 J/cm^2 UVB or simultaneously to IRA+UVB. After 24 hours cells were harvested, permeabilized, stained with antibodies against CD-95, BID, FLIP$_L$ and Bcl-2 and subjected to FACS analysis. Histograms show fluorescence intensity (*x axis*) versus cell number (*y axis*). Percentages indicate positive cells. For each protein one representative experiment is shown.